V.A. ZHOVTYANSKY,[1] O.V. ANISIMOVA [2]

[1] Gas Institute, National Academy of Sciences of Ukraine
  (39, Degtyarivs'ka Str., Kyiv 03113, Ukraine; e-mail: zhovt@ukr.net)
[2] National Technical University of Ukraine "Kyiv. Politekhn. Inst."
  (37, Peremogy Ave., Kyiv 03056, Ukraine)

PACS 51.50.+v, 52.25.Dg, 52.80.Hc

KINETICS OF PLASMA CHEMICAL REACTIONS PRODUCING NITROGEN ATOMS IN THE GLOW DISCHARGE IN A NITROGEN–ARGON GAS MIXTURE

The problem of determining the content of nitrogen atoms in the low-pressure glow discharge (GD) plasma in a nitrogen–argon gas mixture has been considered. The balance of the nitrogen atomic concentration includes for the generation of nitrogen atoms in the course of the molecular nitrogen dissociation by the electron impact, the interaction of nitrogen molecules with metastable Ar, and the loss of nitrogen atoms in the diffusion process followed by the heterogeneous recombination at a GD cathode. The influence of the gas mixture composition on the atomic nitrogen generation is determined by numerical calculations, whereas the plasma parameters are found experimentally using the probe method. The electron energy distribution is determined by numerically integrating the Boltzmann equation written in the binomial approximation for a mixture of molecular nitrogen and argon.

K e y w o r d s: glow discharge, plasma chemical reactions, diffusion processes, Boltzmann equation, probe diagnostics, atomic nitrogen.

1. Introduction

One of the methods aimed at improving the properties of constructional materials is the thermochemical treatment of their surfaces; in particular, this is nitriding, which provides higher hardness, wear resistance, fatigue strength, and corrosion stability [1]. Technologically, the method consists in saturating the near-surface layer of metal products by nitrogen. In the case of the traditional nitriding, the products are heated up in furnaces in the ammonia atmosphere at a temperature of 500–600 °C. During the process, ammonia molecules partially dissociate into atomic hydrogens and nitrogens. The latter are adsorbed by the metal surface and diffuse into the crystal latticem by consecutively forming nitrogenous phases in the metal depth. In essence, these are those phases that provide special properties to the modified surface of the metal.

The plasma methods of nitriding are based on the interaction of atomic nitrogen particles obtained in a low-temperature plasma of a given composition with the metal surface [2]. From the viewpoint of general thermochemical methods, plasma in this case is a technological saturating atmosphere, which affects the surface of a treated metal. Plasma can be produced, in particular, in an abnormal glow discharge (GD) obtained in a rarefied atmosphere of nitrogen or its mixtures with other gases; the most probably, with argon. The advantages of GD include the maximum uniformity of a technological action on the surface of a treated details, even if the surface has a complicated geometrical shape with concave sections. The uniformity is reached when the details are treated in the cathode regime: under the conditions of abnormal GD, unlike the normal one, the cathode spot ex-
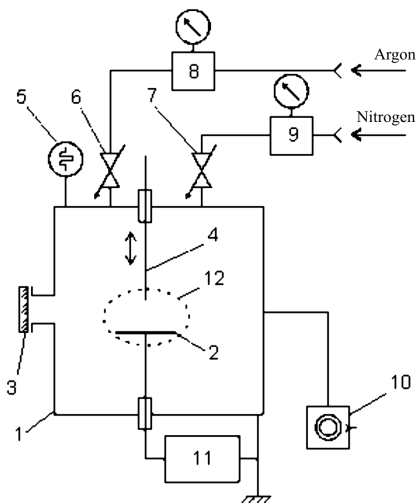
Fig. 1. Schematic diagram of an installation for nitriding in the glow discharge: (*1*) vacuum chamber, (*2*) object stage, (*3*) observation window, (*4*) probe, (*5*) manometric transducer PMT-6-3, (*6, 7*) dosing valves, (*8, 9*) pressure regulators, (*10*) forevacuum pump, (*11*) discharge power unit, (*12*) working zone of discharge

tends over the whole details surface. A cathode layer with a high potential drop between the GD plasma and the details surface is formed at this spot. Besides that this potential is a source of plasma formation, it also maintains two important technological functions by considerably accelerating ions toward the product-cathode. First, this is an effective cleaning of the surface by bombarding ions (this preliminary stage precedes the stage to nitriding in the rarefied argon atmosphere). Second, this is the heating of products to the temperature $T_k = 810 \div 820$ K, which is important for the process of nitriding in their near-surface volume to be optimal.

In the last years, atomic nitrogen – in particular, in a metastable state – is considered to play a dominant role in the diffusion saturation of the metal surface with nitrogen [3, 4]. For this reason, we study the plasma-forming mixtures of nitrogen with an argon admixture, which favors the efficient generation of nitrogen atoms [5]. In our previous works [6,7], the conditions required for the maximum efficiency of the nitriding process were estimated from the viewpoint of the optimization of the component ratio in a mixture. In this work, a further specification was carried out for the plasma chemical reactions of atomic nitrogen formation. In addition, the diffusion losses of

atomic nitrogen in the general balance of the process are taken into account.

2. Object of Research

2.1. Phenomenology of the nitriding process

In this work, the processes responsible for the formation of a technological atmosphere in the course of nitriding are analyzed with regard for the operational features of a used technological installation [2], and the analysis is partially based on the experimental results obtained on it. The installation included a vacuum chamber 50 cm in diameter and of the same height. At the center of the chamber volume, we mounted a molybdenum object stage 4 cm in diameter used for the arrangement of specimens to be treated; the latter, together with the stage, composed a cathode (Fig. 1). The stage temperature was measured by a built-in chromel-alumel thermocouple. The vacuum chamber case played the role of the anode. The electron concentration N_e and the electric field strength E were determined with the help of a double probe, which was moved along the chamber radius (the strength E was measured using the compensation technique). Specimens were nitrided in a nitrogen-argon gas mixture with that or another component ratio at a pressure of 150 Pa and the rate of mixture pumping $q = 1.5$ Pa $\times$ m^3/s. The object stage and, accordingly, the specimen temperature were maintained within the working interval $T_k = 810 \div 820$ K by means of the Joule energy released by the discharge at a power level of 60 W.

The observable region of GD was concentrated in a layer located near the cathode; with the maximum of the electron concentration being located at a distance of 2.5 cm from its surface. Afterward, the magnitude of N_e was gradually decreased. Therefore, this region can be considered as giving the main contribution to the generation of atomic nitrogen, so that it can be regarded as a working zone for the technological process of nitriding.

The dominant role in the diffusion-driven saturation of the metal surface with nitrogen belongs to nitrogen atoms, in particular, in a metastable state [4]. Therefore, the final efficiency of the technological nitriding process should be governed, first of all, by the concentration of atomic nitrogen, N_N. In the low-pressure GD, a considerable role in the gas dissociation, as well as in its ionization and excitation, is

played by the processes of direct electron impact, the rate of which is determined by the discharge parameters; first of all, these are the field strength E and the electron concentration N_e. Those parameters can be determined with the use of the fluid simulation methods, which provided good results when used to find the current-voltage characteristics of GD [8,9]. In particular, they allowed the temperature nonuniformity of the discharge along its radius, which is induced by a relatively high cathode temperature T_k, to be taken into account adequately [10]. In work [11], in the framework of this approach, the coordinate dependences of E and N_e were obtained for the conditions specific to our experiment. However, those researches were restricted to pure gases with the known Townsend coefficients. At the same time, in our case, the research essentially concerned a gas mixture.

2.2. Glow discharge structure

The fluid model is also not able to adequately describe the physical processes in the whole near-cathode discharge region, which includes the cathode layer itself and the negative glow zone [12, Chap. 6]. This is a result of the so-called nonlocal effects, because the electrons acquire a high energy in the cathode layer and effectively make ionization even in the negative glow zone, which is not described by the fluid model.

We should also take into account that the GD considered in the spherical model is confined in the external, with respect to the working zone, part by the Faraday dark space immediately contacting with the anode [12, p. 346]. Therefore, even if the matter concerns the positive column in a spherical GD (see works [8,9]), the region that provides a discharge current connection to the anode located outside the negative glow zone is only a formal issue. At the same time, there is no necessity for the emergence of a positive column from the physical viewpoint, because its role in the ordinary discharges maintained in rather long cylindrical tubes consists in compensating the losses of charged particles at tube walls owing to the ionization of a plasma-forming compound at a level sufficient for maintaining the passage of a discharge current.

As was shown in work [9], under our conditions, the diffusion-driven electron flow to the anode is much lower than the drift one. This is an essential issue, because, otherwise, the electric field in the interelec-
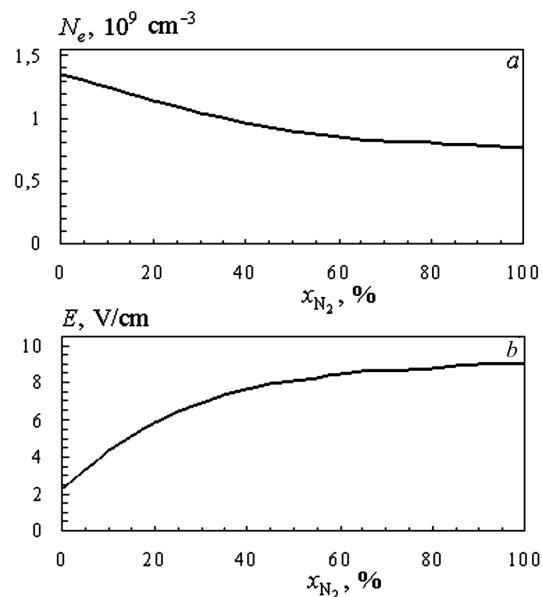
Fig. 2. Dependences of (a) the average electron concentration N_e and (b) the maximum strength of the electric field E in the working zone of GD on the nitrogen content x_{N_2} in a plasma-forming mixture nitrogen–argon

trode gap would change its sign [12, chap. 6], so that the probe measurements would not have any sense at all in the proposed formulation of the problem.

Hence, in this work, as was done earlier in works [6, 7], the values of E and N_e averaged over the working zone [12] (see Fig. 1) are used, while determining the concentration N_N. Their dependences on the nitrogen content x_{N_2} in the technological atmosphere ($x_{N_2} = N_{N_2}/N_g$, where N_{N_2} is the concentration of nitrogen molecules and N_g the total concentration of neutral components) obtained from the results of probe measurements are depicted in Fig. 2.

2.3. Reactions of nitrogen atom formation

In the cited works, the reaction of N_2 dissociation by the electron impact,

$$N_2 + e \rightarrow N + N + e, \tag{1}$$

was considered as the only process of atomic nitrogen formation. The concentration N_N was determined from the balance equation, and the corresponding constant of dissociation rate was found from the electron energy distribution function (EEDF) depending on the field E. Mixing nitrogen with an inert gas stimulates such changes in the EEDF that the fraction of

electrons with energies of about 10 eV, which are sufficient for initiating reaction (1), considerably grows [13, p. 77]. This is the main effect obtained, while adding argon to nitrogen to form technological atmospheres.

However, besides the dissociation by means of the direct electron impact, an appreciable contribution to the generation of atomic nitrogen can be made by other mechanisms as well, the role of which in this process is not evident. In particular, a substantial probability in the case of a nitrogen-argon gas mixture is inherent to the interaction of argon in a metastable state with molecular nitrogen [14], which is an additional source of the atomic nitrogen formation (an analog of the Penning effect for dissociation). The role of this mechanism in the formation of a technological atmosphere is also studied in this work. It is reduced to the influence of argon in the metastable states $Ar^*(^3P_2)$ and $Ar^*(^3P_0)$ with the excitation energies $\Delta\varepsilon_1 = 11.55$ eV and $\Delta\varepsilon_2 = 11.72$ eV, respectively, in the reactions

$$N_2 + Ar^*(^3P_2) \rightarrow N + N + Ar(4S), \qquad (2)$$

$$N_2 + Ar^*(^3P_0) \rightarrow N + N + Ar(4S). \qquad (3)$$
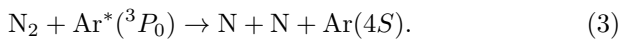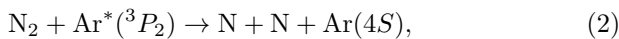
At the same time, the process of excitation by the electron impact is considered as the main one for the formation of metastable argon,

$$Ar + e \rightarrow Ar^* + e. \qquad (4)$$

Among the channels of excited argon losses, we consider the working gas pumping; the quenching of Ar^* by own atoms, molecular nitrogen, or at collisions with electrons; and the diffusion processes on the cathode surface.

A characteristic feature in the structure of excited states in the $3p^5 4s$ configuration of an argon atom should be emphasized. It consists in the mutual proximity of the metastable, $^3P_2$ and $^3P_0$, and resonance, $^3P_1$ and $^1P_1$, levels, which are located in the atomic energy structure forming the sequence $^3P_2$–$^3P_1$–$^3P_0$–$^1P_1$ with the energy intervals of about 0.1 eV [14]. It is believed that this proximity makes transitions from metastable atomic states to resonance ones due to collisions with electrons to be easy under the GD conditions. This circumstance can either give rise to a rapid deexcitation of metastable levels owing to a transition to one of resonance levels followed by

radiation emission or, if the resonance radiation is absorbed, govern the behavior of resonance levels, which becomes similar to that of metastable ones [15]. Using the literature data [16], it can be demonstrated that, under the GD conditions relevant to this work, the self-absorption coefficients for the resonance lines of argon atoms at 106.7 and 104.8 nm amount to $\kappa_0 \approx 5 \times 10^3$ cm^{-1}, so that the probabilities of their glow equal [17, 18]

$$A_{21}^* = 2A_{21}/\tau_0 \approx 2 \times 10^4 \text{ s}^{-1}, \qquad (5)$$

where $\tau_0 = \kappa_0 L$ is the optical thickness of a plasma, and A_{21} the probability of resonance transitions. As a result, the characteristic time of the resonance level depopulation at radiation emission processes amounts to about 0.5×10^{-4} s. The rate of this process is rather high and, in principle, it could be very substantial, provided that this process is not slowed down by the previous stage (the atomic excitation by the electron from the metastable state to the resonance one), the frequency of which equals [19]

$$\omega_{ik} = N_e \sigma_{ik} \left(\frac{kT_e}{m_e}\right)^{1/2} \exp\left(-\frac{\Delta E_{ik}}{kT_e}\right), \qquad (6)$$

where σ_{ik} is the average excitation cross-section, k the Boltzmann constant, T_e the electron temperature, and m_e the electron mass. The process is possible if the kinetic energy of the electron exceeds the excitation energy ΔE_{ik}. Taking into account that, under the GD conditions, $kT_e \sim 1$ eV and the energy difference between the resonance and metastable levels $\Delta E_{ik} \sim 0.1$ eV only, the influence of the exponential factor is insignificant here. For a quantitative evaluation, it is enough to take literature data for the rate constant of this process. For argon, this is about 10^{-7} cm^3/s [14, p. 51]; accordingly, at $N_e \sim 10^9$ cm^{-3}, the characteristic frequency $\omega_{ik} \sim 10^2$ s^{-1}. Ultimately, this value is responsible for the low total rate of the deexcitation of metastable levels through the resonance ones.

According to the data of work [14, pp. 62 and 65], the rate constants of Ar^* quenching by molecular nitrogen are four orders of magnitude larger than if by own atoms. The calculation testifies that, under the experiment conditions when the nitrogen content $x_{N_2} \geqslant 5\%$, the quenching by molecular nitrogen dominates over all other factors, with the corresponding

characteristic time being equal to

$$\tau_{\mathrm{Ar*N_2}} = (K_{\mathrm{Ar*N_2}} N_g x_{\mathrm{N_2}})^{-1}, \qquad (7)$$

where $K_{\mathrm{Ar*N_2}}$ is the quenching rate constant. The latter equals 5.9×10^{-11} cm^3/s for Ar*($^3P_2$) and 2.6×10^{-11} cm^3/s for Ar*($^3P_0$). Assuming also that the dependence $K_{\mathrm{N_2}} \sim \sqrt{T}$ holds true for the transition within the temperature interval from room temperature to T_k, we obtain the following final values for both metastable argon levels at $x_{\mathrm{N_2}} = 0.05$: $\tau_{\mathrm{Ar*}(^3P_2)\mathrm{N_2}} = 2.3 \times 10^{-5}$ s and $\tau_{\mathrm{Ar*}(^3P_0)\mathrm{N_2}} = 5.7 \times \times 10^{-5}$ s. The cumulative contribution of other factors is less than a percent.

Hence, the balance equation for each metastable level Ar* can be written in the form

$$r_{\mathrm{Ar*}} N_e N_{\mathrm{Ar}} = K_{\mathrm{Ar*N_2}} N_{\mathrm{N_2}} N_{\mathrm{Ar*}}, \qquad (8)$$

where $N_{\mathrm{Ar*}}$ and $r_{\mathrm{Ar*}}$ are the concentration and the excitation rate constant, respectively, for the corresponding Ar* level, and N_{Ar} is the argon concentration.

The rates of atomic nitrogen generation owing to the reaction with metastable argon and the electron impact are determined as

$$S_{\mathrm{NAr*}} = 2\eta K_{\mathrm{Ar*N_2}} N_{\mathrm{N_2}} N_{\mathrm{Ar*}} = 2\eta r_{\mathrm{Ar*}} N_e N_{\mathrm{Ar}}, \qquad (9)$$

where η is the dissociation probability at the Ar* quenching, and r_d is the rate constant of dissociation by the direct electron impact.

The final expression of the balance equation for the concentration of nitrogen atoms N_{N} looks like

$$2 r_d N_e N_{\mathrm{N_2}} + 2\eta_1 r_{\mathrm{Ar*}(^3P_2)} N_e N_{\mathrm{Ar}} +$$

$$+ 2\eta_2 r_{\mathrm{Ar*}(^3P_0)} N_e N_{\mathrm{Ar}} = \frac{N_{\mathrm{N}}}{\tau}, \qquad (10)$$

where τ is the average time of the atomic nitrogen stay in the discharge. Hence, the concentration of atomic nitrogen can be determined from the relation

$$N_{\mathrm{N}} = 2\tau N_e N_g \times$$

$$\times \left(r_d x_{\mathrm{N_2}} + \eta_1 r_{\mathrm{Ar*}(^3P_2)} x_{\mathrm{Ar}} + \eta_2 r_{\mathrm{Ar*}(^3P_0)} x_{\mathrm{Ar}} \right), \qquad (11)$$

where $x_{\mathrm{Ar}} = N_{\mathrm{Ar}}/N_g$ is the argon content.

2.4. Electron energy distribution function

In terms of the EEDF, the reaction rate constants are expressed as follows:

$$r_d = \sqrt{\frac{2e}{m_e}} \int\limits_0^\infty \varepsilon \sigma_d(\varepsilon) f_0(\varepsilon) d\varepsilon, \qquad (12)$$

$$r_{\mathrm{Ar*}(^3P_2)} = \sqrt{\frac{2e}{m_e}} \int\limits_0^\infty \varepsilon \sigma_{\mathrm{Ar*}(^3P_2)}(\varepsilon) f_0(\varepsilon) d\varepsilon, \qquad (13)$$

$$r_{\mathrm{Ar*}(^3P_0)} = \sqrt{\frac{2e}{m_e}} \int\limits_0^\infty \varepsilon \sigma_{\mathrm{Ar*}(^3P_0)}(\varepsilon) f_0(\varepsilon) d\varepsilon, \qquad (14)$$

where e is the elementary charge; ε the electron energy; σ_d, $\sigma_{\mathrm{Ar*}(^3P_2)}$, and $\sigma_{\mathrm{Ar*}(^3P_0)}$ are the collision cross-sections of the corresponding processes; and $f_0(\varepsilon)$ is the EEDF normalized by the condition $\int_0^\infty \sqrt{\varepsilon} f_0(\varepsilon) d\varepsilon = 1$. The function $f_0(\varepsilon)$ is found by numerically integrating the Boltzmann equation written in the binomial approximation,

$$\frac{1}{N_e N_g} \left(\frac{m_e}{2e} \right)^{1/2} \varepsilon^{1/2} \frac{\partial (N_e f_0)}{\partial t} -$$

$$- \frac{1}{3} \left(\frac{E}{N_g} \right)^2 \frac{\partial}{\partial \varepsilon} \left(\frac{\varepsilon}{x_{\mathrm{N_2}} \sigma_{\mathrm{N_2}T} + (1 - x_{\mathrm{N_2}}) \sigma_{\mathrm{Ar}T}} \frac{\partial f_0}{\partial \varepsilon} \right) -$$

$$- \frac{\partial}{\partial \varepsilon} \left[2 \left(\frac{m_e}{M_{\mathrm{N_2}}} x_{\mathrm{N_2}} \sigma_{\mathrm{N_2}T} + \frac{m_e}{M_{\mathrm{Ar}}} (1 - x_{\mathrm{N_2}}) \sigma_{\mathrm{Ar}T} \right) \times$$

$$\times \varepsilon^2 \left(f_0 + T \frac{\partial f_0}{\partial \varepsilon} \right) \right] = S_{eN} + A, \qquad (15)$$

where $M_{\mathrm{N_2}}$ and M_{Ar} are the masses of a nitrogen molecule and an argon atom, respectively, $\sigma_{\mathrm{N_2}T}$ and $\sigma_{\mathrm{Ar}T}$ are the corresponding transport cross-sections, and T is the gas temperature. The integral of inelastic collisions with atoms and gas molecules is determined as follows:

$$S_{eN} = \sum_j x_j \big[(\varepsilon + \varepsilon_j) \sigma_j (\varepsilon + \varepsilon_j) \times$$

$$\times f_0(\varepsilon + \varepsilon_j) - \varepsilon \sigma_j(\varepsilon) f_0(\varepsilon) \big],$$

where σ_j are the excitation cross-sections of electron and vibrational nitrogen levels, electron argon levels, and nitrogen dissociation; ε_j the transition energies; and x_j the contents of the corresponding components. The ionization term $A = \sum_j A_j$ includes two

terms corresponding to the argon and nitrogen ionization and looks like

$$A_j = x_j \left(\int\limits_{2\varepsilon+\varepsilon_i}^{\infty} \varepsilon' f_0(\varepsilon') \sigma_i(\varepsilon', \varepsilon) d\varepsilon' + \right.$$

$$\left. + \int\limits_{\varepsilon+\varepsilon_i}^{2\varepsilon+\varepsilon_i} \varepsilon' f_0(\varepsilon') \sigma_i(\varepsilon', \varepsilon' - \varepsilon_i - \varepsilon) d\varepsilon' - \varepsilon f_0(\varepsilon) \sigma_i(\varepsilon) \right).$$

Here,

$$\sigma_i(\varepsilon, \varepsilon') = \frac{1}{\varepsilon_i} \frac{1}{\arctan\left(\frac{\varepsilon-\varepsilon_i}{2\varepsilon_i}\right)} \frac{\sigma_i(\varepsilon)}{1 + (\varepsilon'/\varepsilon_i)^2}$$

is the differential cross-section of ionization by the electron impact, with ε_i and σ_i being the energy and the ionization cross-section, respectively, of the corresponding component.

2.5. Diffusion of nitrogen atoms

In this work, we took into account that the losses of atomic nitrogen from the working zone can occur as a result of the pumping and owing to its diffusion to the cathode (the product) followed by the heterogeneous recombination. The characteristic time of those losses, τ, is determined from the relation

$$\tau^{-1} = \tau_v^{-1} + \tau_d^{-1}, \tag{16}$$

where $\tau_v = 0.025$ s is the characteristic time of pumping, which is specific to the experiment [6, 7], and

$$\tau_d = \frac{\Lambda^2}{D_{\mathrm{N}}} \tag{17}$$

is the characteristic time of diffusion losses. In formula (17), $\Lambda = 1.77$ cm is the specific diffusion length, which is defined as $\Lambda^2 = L^2/2$ (supposing the working zone to be approximately a plane layer of the thickness $2L$), and D_{N} is the diffusion coefficient for atomic nitrogen. The latter is determined from the formula

$$\frac{1}{D_{\mathrm{N}}} = \frac{x_{\mathrm{N_2}}}{D_{\mathrm{NN_2}}} + \frac{1 - x_{\mathrm{N_2}}}{D_{\mathrm{NAr}}}, \tag{18}$$

where $D_{\mathrm{NN_2}}$ and D_{NAr} are the diffusion coefficients of N atoms in molecular nitrogen and argon, respectively. They can be determined from the data of work [20] by interpolating the energy dependences of the

collision cross-sections presented for separate particles participating in the diffusion at the working temperature $T = 800$ K (the energy $\varepsilon = 0.069$ eV). As a result, we obtain $\sigma_{\mathrm{N_2N_2}} = 4.42 \times 10^{-15}$ cm^2 and $\sigma_{\mathrm{ArAr}} = 3.79 \times 10^{-15}$ cm^2. According to the recommendations of the cited work, $\sigma_{\mathrm{NN_2}} = 0.6\sigma_{\mathrm{N_2N_2}} = 2.65 \times 10^{-15}$ cm^2. In the framework of a simplified collision model, those values enable us to find the last unknown cross-section, $\sigma_{\mathrm{NAr}} = 2.4 \times 10^{-15}$ cm^2.

The diffusion coefficients were determined with the help of the Chapman–Enskog formula

$$D = \frac{3\sqrt{2\pi kT}}{16\sqrt{\mu} N_g \sigma}, \tag{19}$$

where μ is the reduced mass, and σ the averaged collision cross-section. The sought quantities were found to equal $D_{\mathrm{NN_2}} = 1.24 \times 10^3$ cm^2/s and $D_{\mathrm{NAr}} = 1.15 \times 10^3$ cm^2/s. The validity of this approach is testified by the complete correspondence of one of those parameters, $D_{\mathrm{NN_2}}$, to the experimental results of work [21] obtained under the same temperature conditions, $D_{\mathrm{NN_2}} = (1.26 \div 1.43) \times 10^3$ cm^2/s.

Making allowance for all data obtained, we obtain that the characteristic time of diffusion losses amounts to $\tau_d = (2.5 \div 2.8) \times 10^{-3}$ s, depending on the component ratio. Hence, the diffusion processes play the crucial role in the total losses of atomic nitrogen.

3. Results

The processes that were taken into consideration while determining the EEDF are listed in Table 1. Unlike works [6, 7], the excitation of argon levels $^3P_2, ^3P_1, ^3P_0,$ and $^1P_1$ in the processes of collision with electrons is taken into account separately. Figure 3 exhibits the EEDFs calculated for various component ratios in the nitrogen–argon gas mixture. The EEDF shape is typical of a nitrogen plasma: it demonstrates a sharp drop at about 2 eV, which corresponds to the threshold energy of the vibrational excitation of nitrogen. However, in general, the results differ from those obtained in works [6, 7], because, as was already indicated, other data concerning the cross-sections of collision processes were used in some cases. As the argon content becomes larger (i.e. at rather low nitrogen contents, see Fig. 3), the fraction of electrons with the energy sufficient for the dissociation and the

Comparative list of elementary atomic and molecular processes taken into account at the determination of the EEDF in this and previous works [6, 7], and references to their cross-sections

No.	Processes	Threshold energy, eV	Maximum cross-section (cm^2), source	
			This work	Works [6, 7]
1	$N_2 + e \rightarrow N_2 + e$	–	3.3×10^{-15} [22]	3.3×10^{-15} [22]
2	$N_2 + e \rightarrow N_2(A^3\Sigma_u^+) + e$	6.7	2.6×10^{-17} [23]	2.6×10^{-17} [23]
3	$N_2 + e \rightarrow N_2(a^1\Pi_g) + e$	8.55	3.8×10^{-17} [24]	3.8×10^{-17} [24]
4	$N_2 + e \rightarrow N_2(v),$ $v = 1, ..., 10$	1.5	5.6×10^{-16} [25]	5.6×10^{-16} [25]
5	$N_2 + e \rightarrow N_2^+ + e + e$	15.6	1.95×10^{-16} [26]	1.95×10^{-16} [26]
6	$N_2 + e \rightarrow N + N + e$	9.76	1.72×10^{-16} [27]	1.72×10^{-16} [27]
7	$Ar + e \rightarrow Ar + e$	–	1.45×10^{-15} [28]	1.45×10^{-15} [28]
8	$Ar + e \rightarrow Ar(4s) + e$	11.6	–	4.3×10^{-17} [30]
9	$Ar + e \rightarrow Ar(^3P_2) + e$	11.55	5.0×10^{-18} [29]	–
10	$Ar + e \rightarrow Ar(^3P_1) + e$	11.62	7.7×10^{-18} [29]	–
11	$Ar + e \rightarrow Ar(^3P_0) + e$	11.72	1.0×10^{-18} [29]	–
12	$Ar + e \rightarrow Ar(^1P_1) + e$	11.83	3.18×10^{-17} [29]	–
13	$Ar + e \rightarrow Ar^+ + e + e$	15.8	2.86×10^{-16} [29]	2.53×10^{-16} [31]

excitation of metastable argon levels increases substantially, which results in a growth of the rate constants r_d, $r_{Ar^*(^3P_2)}$ and $r_{Ar^*(^3P_0)}$ (see Fig. 4).

Figure 5 illustrates the values of atomic nitrogen concentration N_N calculated making use of the above-stated values of N_e, r_d, $r_{Ar^*(^3P_2)}$, and $r_{Ar^*(^3P_0)}$ (curve *1*). For comparison, the results of calculation in the case where the N_2 dissociation reaction is governed only by the N_2 collision with an electron are also depicted (curve *2*). One can draw conclusion that, at nitrogen contents lower than 30%, the channel of N formation through metastable argon gives an appreciable contribution to the atomic nitrogen generation. In both cases, each obtained dependence of the atomic nitrogen concentration N_N on the nitrogen content x_{N_2} reveals a maximum. In other words, an x_{N_2}-value corresponding to the optimum nitriding regime can be found. In case 1, the maximum concentration N_{Nmax} is appreciably higher and a little shifted toward lower x_{N_2}-values, which corresponds, in general, to experimental results [2].

It is essential that, as a rule, the concentration of atomic nitrogen calculated in this work is an order of magnitude lower in comparison with the results of works [6, 7]. For instance, $N_{Nmax} = 3.8 \times 10^{11}$ cm^{-3} in this work (Fig. 5, curve *2*), whereas $N_{Nmax} = 3.6 \times 10^{12}$ cm^{-3} in the previous works. This fact is
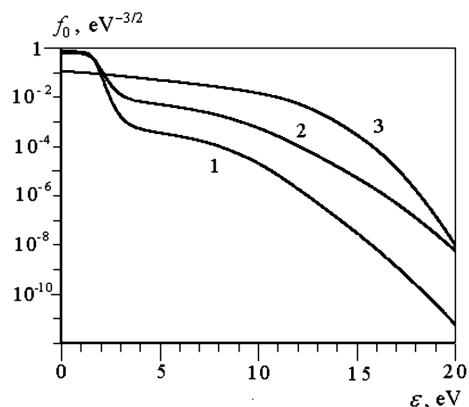
Fig. 3. Electron energy distribution functions for various nitrogen contents $x_{N_2} = 1$ (*1*), 0.5 (*2*), and 0 (*3*)

associated with the influence of diffusion losses, the characteristic time of which, τ_d, is an order of magnitude less than the pumping time τ_v.

It is significant that the rate of atomic nitrogen generation, which is determined by the interaction with metastable argon, does not depend on the concentration of molecular nitrogen in a wide interval of x_{N_2}. This circumstance is connected with the fact that argon in the metastable state effectively interacts with molecular nitrogen and quickly transits into the ground state. Therefore, the rate of nitrogen dis-
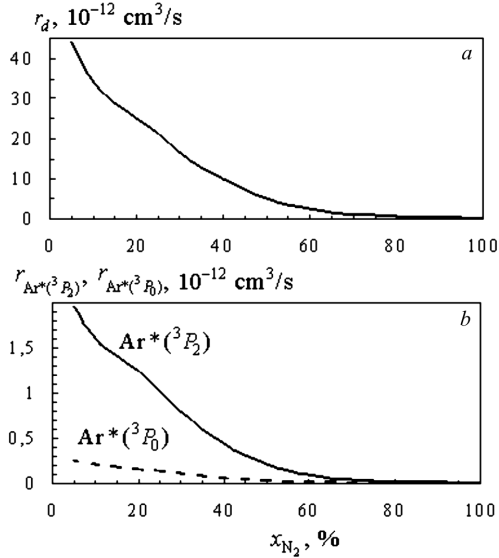
Fig. 4. Dependences of the rate constants (*a*) r_d and (*b*) $r_{\mathrm{Ar}^*(^3P_2)}$ and $r_{\mathrm{Ar}^*(^3P_0)}$ on the nitrogen content x_{N_2} in a plasma-forming mixture nitrogen–argon
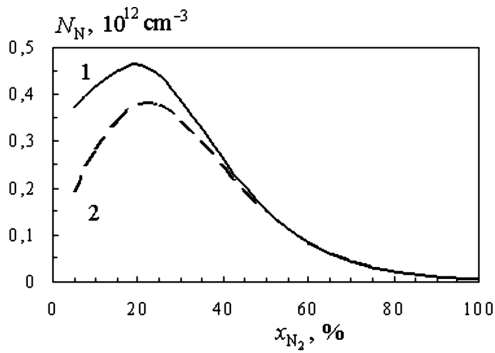
Fig. 5. Influence of the nitrogen content x_{N_2} in a plasma-forming mixture nitrogen–argon on the atomic nitrogen concentration N_{N} calculated with regard for (*1*) the dissociation processes with the participation of $\mathrm{Ar}^*(^3P_2)$ and $\mathrm{Ar}^*(^3P_0)$ and (*2*) the dissociation by electron impact only

sociation through metastable argon is determined by the rate of argon excitation by electrons. As a result, the influence of this mechanism manifests itself more strongly at lower nitrogen contents x_{N_2} (see Fig. 5).

At last, it is worth noting that, in expression (11), we implicitly took the probability of dissociation at the Ar^* quenching to be $\eta_1 = \eta_2 = \eta = 1$. At the same time, the quenching process can also run by transferring the excitation from argon atoms to the vibrational levels of nitrogen molecules [32]. However,

as was marked in the recent work [33], there are few quantitative data that characterize both variants of the Ar^* quenching; in addition, they are inconsistent. Therefore, we used the data of work [32] for argon in the metastable state $\mathrm{Ar}^*(^3P_2)$, namely, the excitation cross-section of vibrational nitrogen levels $C^3\Pi_u$ and the total quenching cross-section, because its influence on the processes studied in this work dominates. The corresponding values equal 4×10^{-16} cm^{-2} and 7×10^{-16} cm^{-2}, respectively, at a total measurement error of 50%. We also obtained a basis to evaluate the influence of the nitrogen content x_{N_2} in the plasma-forming mixture nitrogen–argon on the atomic nitrogen concentration N_{N} making allowance for the dissociation processes with the participation of $\mathrm{Ar}^*(^3P_2)$ and $\mathrm{Ar}^*(^3P_0)$ at $\eta_1 = \eta_2 = \eta = 0.5$ by analogy with Fig. 5. In the latter case, the magnitude of N_{Nmax} for curve 1 in Fig. 5 decreases from 4.6×10^{11} cm^{-3} to 4.2×10^{11} cm^{-3}, and the corresponding functional dependence acquires intermediate values between curves *1* and *2* in Fig. 5.

4. Conclusion

On the one hand, the obtained results additionally confirm the crucial role of atomic nitrogen in the processes of metal surface nitriding. On the other hand, they can be used for simulating those processes and their optimization.

1. A.K. Minkevich, *Thermochemical Treatment* (Mashinostroenie, Moscow, 1968) (in Russian).
2. O.G. Didyk, V.A. Zhovtyansky, V.G. Nazarenko, and V.O. Khomych, Ukr. J. Phys. **53**, 482 (2008).
3. V.A. Zhovtyansky, Ukr. J. Phys. **53**, 490 (2008).
4. T. Kitajima, T. Nakano, and S. Samukawa, Plasma Sources Sci. Technol. **17**, 1 (2008).
5. D.I. Slovetskii, Khim. Plazmy No. 1, 156 (1974).
6. V.A. Khomich, A.V. Ryabtsev, E.G. Didyk, V.A. Zhovtyansky, and V.G. Nazarenko, Tech. Phys. Lett. **36**, 918 (2010).
7. V.A. Khomich, A.V. Ryabtsev, E.G. Didyk, V.A. Zhovtyansky, and V.G. Nazarenko, Fiz. Khim. Obrab. Mater. No. 2, 44 (2012).

8. V.A. Zhovtyansky and Yu.I. Lelyukh, Ukr. J. Phys. **53**, 497 (2008).

9. V.A. Zhovtyansky and Yu.I. Lelyukh, Tech. Phys. Lett. **35**, 725 (2009).

10. V.A. Zhovtyansky, O.V. Anisimova, V.O. Khomych, Yu.I. Lelyukh, V.G. Nazarenko, and Ya.V. Tkachenko, Probl. At. Sci. Techn. **1**, 95 (2011).

11. V.A. Zhovtyansky, V.G. Nazarenko, V.O. Khomych, A.V. Ryabtsev, O.V. Anisimova, I.O. Nevzglyad, and O.Ya. Shnyt, Probl. At. Sci. Techn. **1**, 92 (2011).

12. A.A. Kudryavtsev, A.S. Smirnov, and L.D. Tsendin, *Physics of Glow Discharge* (Lan', St.Petersburg, 2010) (in Russian).

13. D.I. Slovetskii, *Mechanisms of Chemical Reactions in Nonequilibrium Plasma* (Nauka, Moscow, 1980) (in Russian).

14. B.M. Smirnov, *Excited Atoms* (Energoatomizdat, Moscow, 1982) (in Russian).

15. *Principles of Laser Plasma*, edited by G. Bekefi (Wiley, New York, 1976).

16. A.A. Radtsig and B.M. Smirnov, *Reference Data on Atoms, Molecules, and Ions* (Springer, Berlin, 1986).

17. R. Mewe, Brit. J. Appl. Phys. **18**, 107 (1967).

18. C. Breton and J.-L. Schwob, C. R. Acad. Sci. Paris **260**, 461 (1965).

19. L.M. Biberman, V.S. Vorob'ev, and I.T. Yakubov, *Kinetics of Nonequilibrium Low-Temperature Plasmas* (Consultants Bureau, New York, 1987).

20. A V. Phelps, J. Phys. Chem. Ref. Data **20**, 557 (1991).

21. J.E. Morgan and H.I. Schiff, Can. J. Chem. **42**, 2300 (1964).

22. A.V. Yeletskii, L.A. Palkina, and B.M. Smirnov, *Transfer Phenomena in Weakly Ionized Plasma* (Atomizdat, Moscow, 1975) (in Russian).

23. C.J. Gillant, J. Tennyson, B.M. McLaughlin, P.G. Burke, J. Phys. B **29**, 1531 (1996).

24. J.M. Ajello, J. Chem. Phys. **53**, 1156 (1970).

25. M. Vicic, G. Poparic, and D.S. Belic, J. Phys. B **29**, 1273 (1996).

26. H.C. Straub, P. Renault, B.G. Lindsay, K.A. Smith, and R.F. Stebbings, Phys. Rev. A **54**, 2146 (1996).

27. H.F. Winters, J. Chem. Phys. **44**, 1472 (1966).

28. L.S. Frost and A.V. Phelps, Phys. Rev. **136**, A1538 (1964).

29. ftp://jila.colorado.edu/collision_data.

30. A.A. Mityureva and V.V. Smirnov, J. Phys. B **27**, 1869 (1994).

31. H.A. Hyman, Phys. Rev. A **20**, 855 (1979).

32. O.P. Bochkova, N.V. Tchernysheva, and Yu.A. Tolmachev, Opt. Spektrosk.**36**, 36 (1974).

33. T.H. Chung, Y.W. Lee, H.M. Joh, and M.A. Song, AIP Advances **1**, 032136 (2011).

В.А. Жовтянський, О.В. Анісімова

КІНЕТИКА ПЛАЗМОХІМІЧНИХ РЕАКЦІЙ
УТВОРЕННЯ АТОМІВ АЗОТУ В ЖЕВРІЮЧОМУ
РОЗРЯДІ В СУМІШІ АЗОТ–АРГОН

Р е з ю м е

Розглянуто задачу визначення вмісту атомарного азоту як активної компоненти, відповідальної за ефективність технологій модифікації поверхні металів у плазмі стаціонарного жевріючого розряду (ЖР) низького тиску в суміші азот–аргон, широко застосовуваній у цих технологіях. Баланс концентрації атомів азоту включає їхню генерацію дисоціацією прямим електронним ударом молекулярного азоту та взаємодією останнього з аргоном у метастабільних станах і втрати у дифузійних процесах з подальшою гетерогенною рекомбінацією на катоді ЖР. Вплив складу суміші на продукування атомарного азоту визначався розрахунковим шляхом, а параметри плазми – експериментально, зондовим методом. Функція розподілу електронів за енергіями визначалась чисельним інтегруванням рівняння Больцмана, записаного в двочленному наближенні для суміші молекулярного азоту й аргону.